Applied Mathematics & Information Sciences
An International Journal

http://dx.doi.org/10.18576/amis/180607

Exploring the Impact of Endoscope, Jeffrey Fluid, Magnetic Field, and Separated Flow on Peristaltic Motion in Non-Uniform Tubes

E. G. El-Hadidy[1,*], *M. Ibrahim*[1], *Mohammad Hafez*[2], *Shawkat Alkhazaleh*[3], *and Abd El Hakeem Abd El Naby*[1]

[1]Mathematics Department, Faculty of Science, Damietta University, Damietta, Egypt
[2]Department of Civil Engineering, Faculty of Engineering, FEQS, INTI-IU UNiversity, Nilai, Malaysia
[3]Department of Mathematics, Faculty of sciences and information technology, Jadara University, Irbid, Jordan

Received: 12 May 2024, Revised: 2 Jul. 2024, Accepted: 12 Jul. 2024
Published online: 1 Nov. 2024

Abstract: This paper investigates the behavior of an incompressible Jeffrey fluid flowing between an inner and an outer tube. The inner tube represents an endoscope, while the outer tube has a non-uniform shape with a sinusoidal wave on its wall. A radial magnetic field is present. The analysis utilizes cylindrical coordinates and assumes long wavelength and low Reynolds number approximations. Exact and approximate solutions are obtained using the regular perturbation method. Numerical calculations are performed to determine the pressure rise, frictional force, and pressure gradient, which are then compared graphically. The study discusses trapping phenomena and finds good agreement between the numerical and perturbation results. Overall, the work provides insights into the behavior of the Jeffrey fluid and its interaction with the non-uniform tube and magnetic field.

Keywords: Endoscope, Jeffrey Fluid, Separated Flow, Peristaltic Motion

1 Introduction

The functions of the small intestine in human, which is called gastrointestinal tract, are for digestion and absorption. It is known that endoscopy can be a powerful means in diagnosis and management of various types of intestinal illnesses. A flexible tube called an endoscope is used to view different parts of the digestive tract. The tube contains several channels along its length. The different channels are used to transmit light to the area being examined, to view the area through a camera lens with a camera at the tip of the tube, to pump fluids or air in or out. When passed through the mouth, an endoscope can be used to examine the esophagus, the stomach, and first part of the small intestine. When passed through the anus, an endoscope can be used to examine the rectum and the entire large intestine [1].

The mechanics of peristalsis has been examined by a number of investigators. Rao and Mishra [2] investigated the peristaltic transport of a power-law fluid which accommodates the study of both shear thinning and shear thickening fluids in an axisymmetric porous tube under long wavelength and inertia free approximations. Haroun [3] investigated the peristaltic flow of a third order fluid in an asymmetric channel under the assumptions of long wavelength approximation and the velocity components and the pressure could be expanded in a regular perturbation series in a small parameter Deborah number that contained the non-Newtonian coefficients appropriate to shear-thinning.

The application of magnets to the human body is magnetotherapy that is used to treat the diseases. No drugs are administered under thus therapy. Magnetohydrodynamics (MHD) is the science which deals with the motion of a highly conducting fluids in the presence of a magnetic field. The effect of moving magnetic field on blood flow was studied by Stud et al. [4], they observed that the effect of suitable moving magnetic field accelerates the speed of blood. Srivastava and Agrawal [5] considered the blood as an electrically conducting fluid and constitutes a suspension of red cell in plasma. Agrawal and Anwaruddin [6] studied the effect of magnetic field on blood flow by taking a simple mathematical model for blood through an equally branched channel with flexible walls executing peristaltic

* Corresponding author e-mail: eman_elhadidy82@yahoo.com

waves using long wavelength approximation method and observed, for the flow blood in arteries with arterial disease like arterial stenosis or arteriosclerosis, that the influence of magnetic field may be utilized as a blood pump in carrying out cardiac operations. Also, Hayat et al. [7] discussed the peristaltic flow of a MHD fourth grade fluid in a channel under the consideration of long wavelength and low Reynolds number, and they considered the fluid as electrically conducting in the presence of a uniform transverse magnetic field. Kothandapani et al. [8] studied the influence of applied magnetic field on the peristaltic flow of a Jeffrey fluid in asymmetric channel and different wave forms. Hayat et al. [9] analyzed the influence of applied magnetic field on the peristaltic flow of a Jeffrey fluid in a tube. Hayat et al. [10] analyzed the problem of MHD peristaltic flow of an incompressible Jeffrey fluid in a tube with an endoscope. Reddy et al. [11] studied the effects of magnetic field and slip on the peristaltic flow of a Jeffrey fluid through a porous medium in an asymmetric channel under the assumptions of long wavelength and low Reynolds number.

Nadeem et al. [12] investigated the effects of slip and induced magnetic field on the peristaltic flow of a Jeffrey fluid in an asymmetric channel. Reddy et al. [13] investigated the peristaltic flow of a Jeffrey fluid in a tube with variable viscosity under the assumption of long wavelength. Rajanikanth et al. [14] discussed the effects of partial slip on the peristaltic flow of a Jeffrey fluid in an asymmetric channel under the assumptions of long wavelength and low Reynolds number. Kumari et al. [15] investigated the peristaltic pumping of a Jeffrey fluid in an inclined channel under long wavelength and low Reynolds number assumptions,the magnetic field of uniform strength is applied in the transverse direction to the flow.

Physiological organs are generally observed to be a non-uniform duct [16, 17]. Hence, peristaltic analysis of a Newtonian fluid in a uniform geometry cannot be applied when explaining the mechanism of transport of fluid in most bio-systems. Srivastava et al. [18] have studied peristaltic transport of Newtonian and non-Newtonian fluid in non-uniform geometries. Misra and Pandey [19] analyzed the axisymmetric flow of a viscous incompressible Newtonian fluid through a circular tube of varying cross section when the wave propagating along the wall of the tube is sinusoidal and the initial flow is Hagen- Poiseuille. Elshehawey et al. [20] studied the peristaltic motion of Carreau fluid in a non-uniform channel, and they developed the solution in a perturbation series in powers of Weissenberg number using long wavelength approximation. Mekheimer [21] studied the effect of a uniform magnetic field on peristaltic transport of a blood in a non-uniform two-dimensional channels, when blood is represented by a couple-stress fluid. Also, Elshehawey et al. [22] studied the axisymmetric peristaltic motion of a viscous compressible liquid through a flexible pore of changing cross-section. Mekheimer [23] studied the peristaltic transport of a viscous incompressible fluid (creeping flow) through the gap between coaxial tubes, where the outer tube is non-uniform and has a sinusoidal wave travelling down its wall and the inner one is a rigid, uniform tube and moving with a constant velocity.

There exist several investigators who studied the separated flow (trapping) phenomenon at the center-line of the tube in the cartesian and cylindrical coordinates [24-29]. Abd El Hakeem Abd El Naby et al [30] studied the flow separation on the wall. Also, they found that the trapping region at the wall decreases with increasing volume flow rate and it is observed that the pressure rise and the friction force at the flow separation points are independent approximately of Weissenberg number and power law index at certain values of volume flow rate. Also, the pressure rise and the friction force at the flow separation points increase with increases volume flow rate. Abd El Hakeem Abd El Naby et al [31] investigated the effects of magnetic field on trapping at the centerline and at the channel wall for Carreau fluid through uniform channel using a perturbation method in terms of Weissenberg number, they noted that the pressure rise and friction force for Newtonian and Carreau fluids increase with Hartmann number except at certain values of volume flow rate. The trapping limit and the trapping occurrence region at the center-line increase with Hartmann number but they are independent approximately of Hartmann number at certain values of amplitude ratio. In addition, Abd El Hakeem Abd El Naby et al [32] investigated separation in the flow through peristaltic motion of Power-law fluid in uniform tube, they found that the trapping region at the wall decreases with increasing volume flow rate [36]-[42].

The purpose of this investigation is to study the peristaltic pumping of MHD non-Newtonian Jeffrey fluid through the gap between inner and outer tubes where the inner tube is an endoscope and the outer tube is a non-uniform tube has a sinusoidal wave travelling down its wall in the presence of a radial magnetic field. To the best of our knowledge, this problem has not been investigated yet. We have shown the effect of magnetic field and an endoscope on peristaltic motion of a Jeffrey fluid on peristaltic motion through Non-Uniform peristalsis tubes. Here, the governing equations are nonlinear in nature, we have used infinitely long wave-length assumption to obtain linearized system of coupled differential equations which are then solved analytically. Results have been discussed for pressure rise, friction force on the inner and outer tubes to observe the effect of magnetic field in the presence an endoscope. We have shown the effects of an endoscope and Jeffrey fluid on trapping at boundary of the endoscope and small intestine. The numerical results displayed by figures and the physical meaning is explained.

2 Formulation and analysis

We consider the MHD flow of a Jeffrey fluid through the gap between the inner tube (endoscope) and the outer non-uniform tube which has a sinusoidal wave travelling down its wall. The geometry of the wall surfaces is described as follows:

$$\bar{R}_1 = a_1, \tag{1}$$

$$\bar{R}_2 = a(\bar{Z}) + b\sin\frac{2\pi}{\lambda}(\bar{Z} - c\bar{t}), \tag{2}$$

where

$$a(\bar{Z}) = a_2 + k_0\bar{Z}, \tag{3}$$

where $a(\bar{Z})$ is the radius of the tube at any axial distance $\bar{Z}$ from an inlet, a_1 is the radius of endoscope, a_2 is the radius of the small intestine at the inlet, $k_0 << 1$ is a constant whose magnitude depends on the length of the tube and exit and inlet dimensions, b is the amplitude of the wave, λ is the wavelength, $\bar{t}$ is the time and c is the wave speed. We choose the cylindrical coordinate system $(\bar{R},\bar{Z})$, where the $\bar{Z}$-axis lies along the center-line of the inner and outer tubes and $\bar{R}$ is the distance measured radially.

In the moving coordinates $(\bar{r},\bar{z})$ which travel in the $\bar{Z}$ −direction with the same speed as the wave, the flow can be treated as steady, but if we choose the laboratory frame $(\bar{R},\bar{Z})$, then the flow in the gap between inner and outer tubes is unsteady. The coordinates frames are related through:

$$\bar{Z} = \bar{z} + c\,\bar{t}, \qquad \bar{r} = \bar{R}, \tag{4}$$

$$\bar{W} = \bar{w} + c, \qquad \bar{u} = \bar{U}, \tag{5}$$

where $\bar{U}$,$\bar{W}$ and $\bar{u},\bar{w}$ are the velocity component in the radial and axial directions in the laboratory frame and moving coordinates, respectively.

The constitutive equation for the extra stress tensor $\tilde{S}$ for a Jeffrey fluid is defined by :

$$\tilde{S} = \frac{\mu}{1+\lambda_1}(\tilde{\dot{\gamma}} + \lambda_2\tilde{\ddot{\gamma}})$$

In the above equation, μ is the coefficient of viscosity, λ_1 is the ratio of relaxation to retardation times, $\tilde{\dot{\gamma}}$ the shear rate, λ_2 the retardation time and dots denote the differentiation with respect to time.

The fluid is electrically conducting in the presence of a uniform magnetic field $\bar{B}$ applied transversely to the flow. Under the assumption of low Reynolds number the magnetic body force $\bar{j}\times\bar{B} = -\sigma B_0^2\bar{V}$, where $\bar{V}$ is the fluid velocity vector. By applying these assumptions, the continuity equation and the Navier-Stokes equations

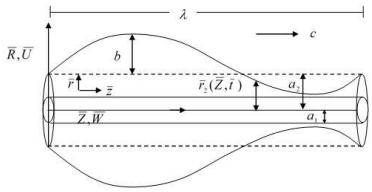

Fig. 1: Effects of endoscope on peristaltic motion

which govern the flow in the stationary coordinates are:

$$\frac{1}{\bar{R}}\frac{\partial(\bar{R}\bar{U})}{\partial\bar{R}} + \frac{\partial\bar{W}}{\partial\bar{Z}} = 0, \tag{6}$$

$$\rho\left(\frac{\partial\bar{U}}{\partial\bar{t}} + \bar{U}\frac{\partial\bar{U}}{\partial\bar{R}} + \bar{W}\frac{\partial\bar{U}}{\partial\bar{Z}}\right) = -\frac{\partial\bar{P}}{\partial\bar{R}} + \frac{\partial}{\partial\bar{R}}\left[\bar{R}\,\tilde{S}_{11}\right] + \frac{\partial\tilde{S}_{31}}{\partial\bar{Z}} - \frac{\tilde{S}_{22}}{\bar{R}}, \tag{7}$$

$$\rho\left(\frac{\partial\bar{W}}{\partial\bar{t}} + \bar{U}\frac{\partial\bar{W}}{\partial\bar{R}} + \bar{W}\frac{\partial\bar{W}}{\partial\bar{Z}}\right) = -\frac{\partial\bar{P}}{\partial\bar{Z}} + \frac{1}{\bar{R}}\frac{\partial}{\partial\bar{R}}\left[\bar{R}\,\tilde{S}_{13}\right] + \frac{\partial\tilde{S}_{33}}{\partial\bar{Z}} - \sigma B_0^2\bar{W}, \tag{8}$$

where ρ is the density, $\bar{P}$ the pressure. The geometry of the wall surfaces are described as Figure(1).

The boundary conditions in the stationary coordinates are:

$$\bar{W} = 0\ ,\bar{U} = 0 \ \text{ at } \ \bar{R} = \bar{R}_1, \tag{9}$$

$$\bar{W} = 0, \bar{U} = \frac{\partial\bar{R}_2}{\partial\bar{t}} \ \text{ at } \ \bar{R} = \bar{R}_2. \tag{10}$$

Using the following non-dimensional variables appearing in above eqs. Introducing Reynolds number (Re) and the wave number (δ) as follows:

$$r = \frac{\bar{r}}{a_2},\ R = \frac{\bar{R}}{a_2},\ r_1 = \frac{\bar{r}_1}{a_2} = \frac{a_1}{a_2} = \varepsilon < 1,$$

$$z = \frac{\bar{z}}{\lambda},\ Z = \frac{\bar{Z}}{\lambda}, S_{ij} = \frac{a_2\tilde{S}_{ij}}{\mu c}$$

$$u = \frac{\lambda\bar{u}}{a_2c},\ U = \frac{\lambda\bar{U}}{a_2c},\ w = \frac{\bar{w}}{c},\ W = \frac{\bar{W}}{c},$$

$$\delta = \frac{a_2}{\lambda} < 1, \qquad \mathrm{Re} = \frac{ca_2\rho}{\mu},$$

$$P = \frac{\bar{P}a_2^2}{c\lambda\mu},\ t = \frac{c\,\bar{t}}{\lambda},\ \phi = \frac{b}{a_2} < 1,$$

$$R_2 = \frac{\bar{R}_2}{a_2} = 1 + \frac{\lambda k_0 Z}{a_2} + \phi\sin 2\pi(Z-t), \tag{11}$$

where ε is the radius ratio, ϕ is the amplitude ratio and μ_0 is the viscosity on the endoscope.

The equations of motion, extra stress components and the boundary conditions in the dimensionless form become:

$$\frac{1}{R}\frac{\partial(RU)}{\partial R} + \frac{\partial W}{\partial Z} = 0, \tag{12}$$

$$\mathrm{Re}\delta^3\left(\frac{\partial U}{\partial t}+U\frac{\partial U}{\partial R}+W\frac{\partial W}{\partial Z}\right)=-\frac{\partial P}{\partial R}+\frac{\delta^2}{R}\frac{\partial(RS_{11})}{\partial R}+\delta^2\frac{\partial S_{31}}{\partial Z}-\delta^2\frac{S_{22}}{R} \quad (13)$$

$$\mathrm{Re}\delta\left(\frac{\partial W}{\partial t}+U\frac{\partial W}{\partial R}+W\frac{\partial W}{\partial Z}\right)=-\frac{\partial P}{\partial Z}+\frac{1}{R}\frac{\partial(RS_{13})}{\partial R}+\delta\frac{\partial S_{33}}{\partial Z}-M^2W \quad (14)$$

where $M=\sqrt{\frac{\sigma}{\mu}}B_0a_2$. The extra stress components of Jeffrey fluid are:

$$\begin{aligned}
S_{11} &= \tfrac{2\delta}{1+\lambda_1}\left[1+\tfrac{c\lambda_2\delta}{a_2}\left(\tfrac{\partial}{\partial t}+U\,\tfrac{\partial}{\partial R}+W\,\tfrac{\partial}{\partial Z}\right)\right]\tfrac{\partial U}{\partial R}\\
S_{13} &= \tfrac{1}{1+\lambda_1}\left[1+\tfrac{c\lambda_2\delta}{a_2}\left(\tfrac{\partial}{\partial t}+U\,\tfrac{\partial}{\partial R}+W\,\tfrac{\partial}{\partial Z}\right)\right]\left(\tfrac{\partial W}{\partial R}+\delta^2\tfrac{\partial U}{\partial Z}\right)\\
S_{22} &= \tfrac{2\delta}{1+\lambda_1}\left[1+\tfrac{c\lambda_2\delta}{a_2}\left(\tfrac{\partial}{\partial t}+U\,\tfrac{\partial}{\partial R}+W\,\tfrac{\partial}{\partial Z}\right)\right]\tfrac{U}{R}\\
S_{33} &= \tfrac{2\delta}{1+\lambda_1}\left[1+\tfrac{c\lambda_2\delta}{a_2}\left(\tfrac{\partial}{\partial t}+U\,\tfrac{\partial}{\partial R}+W\,\tfrac{\partial}{\partial Z}\right)\right]\tfrac{\partial W}{\partial Z}
\end{aligned} \quad (15)$$

with the dimensionless boundary conditions:

$$W=0, U=0 \quad \text{at} \quad R=R_1, \quad (16)$$

$$W=0, U=\frac{\partial R_2}{\partial t} \text{ at } \quad R=R_2. \quad (17)$$

Using the long wavelength approximation ($\delta=0$), then the Navier-Stokes equations and extra-stress components reduce to:

$$\frac{\partial P}{\partial R}=0, \quad (18)$$

$$\frac{\partial P}{\partial Z}=\frac{1}{R}\frac{\partial\,(RS_{13})}{\partial R}-M^2W, \quad (19)$$

$$S_{13}=\frac{1}{1+\lambda_1}\frac{\partial W}{\partial R}, \quad (20)$$

substituting from eq. (20) into eq. (19) we obtained:

$$\frac{\partial P}{\partial Z}=\frac{\kappa^2}{R}\frac{\partial}{\partial R}\left(R\,\frac{\partial W}{\partial R}\right)-M^2W \quad (21)$$

where $\kappa=\frac{1}{\sqrt{1+\lambda_1}}$. The solution of eq. (21) subject to conditions (16) and (17) is :

$$W(R,Z,t)=A_1(Z,t)\,I_0\left(\frac{MR}{\kappa}\right)+A_2(Z,t)\,K_0\left(\frac{MR}{\kappa}\right)-\frac{\frac{\partial P}{\partial Z}}{M^2}, \quad (22)$$

where

$$A_1(Z,t)=\frac{-\left(\frac{\frac{\partial P}{\partial Z}}{M^2}\right)\left(K_0\left(\frac{MR_2}{\kappa}\right)-K_0\left(\frac{MR_1}{\kappa}\right)\right)}{\left(K_0\left(\frac{MR_1}{\kappa}\right)I_0\left(\frac{MR_2}{\kappa}\right)-K_0\left(\frac{MR_2}{\kappa}\right)I_0\left(\frac{MR_1}{\kappa}\right)\right)}, \quad (23)$$

$$A_2(Z,t)=\frac{\left(\frac{\frac{\partial P}{\partial Z}}{M^2}\right)\left(I_0\left(\frac{MR_1}{\kappa}\right)-I_0\left(\frac{MR_2}{\kappa}\right)\right)}{\left(K_0\left(\frac{MR_1}{\kappa}\right)I_0\left(\frac{MR_2}{\kappa}\right)-K_0\left(\frac{MR_2}{\kappa}\right)I_0\left(\frac{MR_1}{\kappa}\right)\right)}, \quad (24)$$

where $I_0\left(\frac{MR_2}{k}\right)$ and $K_0\left(\frac{MR_2}{k}\right)$ are the modified Bessel's functions of first and second kind of order zero respectively. Integrating equation (12) with using equation (22), we get:

$$U(R,Z,t)=\frac{1}{R}\left[\frac{\kappa\,\acute{A}_1(Z,t)\left(R_1I_1\left(\frac{MR_1}{\kappa}\right)-RI_1\left(\frac{MR}{\kappa}\right)\right)}{M}+\frac{\kappa\,\acute{A}_2(Z,t)\,\left(RK_0\left(\frac{MR}{\kappa}\right)-R_1K_0\left(\frac{MR_1}{\kappa}\right)\right)}{M}+\frac{\frac{\partial^2P}{\partial Z^2}}{2M^2}(R^2-R_1^2)\right], \quad (25)$$

where $I_1\left(\frac{MR_2}{k}\right)$ and $K_1\left(\frac{MR_2}{k}\right)$ are the modified Bessel's functions of first and second kind of order one respectively. The rate of volume flow in the stationary and moving coordinates are given by:

$$\bar{Q}(\bar{Z},\bar{t})=2\pi\int_{\bar{R}_1}^{\bar{R}_2(\bar{Z},\bar{t})}\bar{W}\,\bar{R}\,d\bar{R}, \quad (26)$$

$$\bar{q}(\bar{z})=2\pi\int_{\bar{r}_1}^{\bar{r}_2(\bar{z})}\bar{w}\,\bar{r}d\bar{r}. \quad (27)$$

Substituting from eqs. (4) and (5) into eq. (26) and making use of eq. (27) we get:

$$\bar{Q}=\bar{q}+\pi c\,(\,\bar{R}_2^2-\bar{R}_1^2). \quad (28)$$

The time-mean flow over a period $T=\frac{\lambda}{c}$ at a fixed $Z-$position is defined as:

$$\hat{Q}=\frac{1}{T}\int_0^T\bar{Q}(\bar{Z},\bar{t})d\bar{t}. \quad (29)$$

Substituting from eq. (28) in eq. (29) and using eqs. (1) and (2) we obtain:

$$\hat{Q}=\bar{Q}-(2\pi cba_2+2\pi bk_0c\bar{Z})\sin\frac{2\pi}{\lambda}(\bar{Z}-c\bar{t})-\pi cb^2\sin^2\frac{2\pi}{\lambda}(\bar{Z}-c\bar{t})+\frac{\pi cb^2}{2}. \quad (30)$$

On defining the dimensionless time- mean flow Θ and the rate of volume flow F in the stationary coordinates as follows:

$$\Theta=\frac{\hat{Q}}{2\pi ca_2^2} \quad \text{and} \quad F=\frac{\bar{Q}}{2\pi ca_2^2},$$

we obtain:

$$F(Z,t) = \Theta + (1+\frac{\lambda k_0 Z}{a_2})\phi \sin 2\pi(Z-ct) + \frac{\phi^2}{2}\sin^2 2\pi(Z-ct) - \frac{\phi^2}{4}, \tag{31}$$

where

$$F(Z,t) = \int_{R_1}^{R_2} RW dR. \tag{32}$$

Integrating equation (32), with using equation (22), we obtain

$$\frac{\partial P}{\partial Z} = \frac{1}{C}\left[2M^4 F\left(K_0\left(\frac{MR_1}{\kappa}\right)I_0\left(\frac{MR_2}{\kappa}\right) - K_0\left(\frac{MR_2}{\kappa}\right)I_0\left(\frac{MR_1}{\kappa}\right)\right)\right], \tag{33}$$

where

$$C = -4\kappa^2 + M^2\left[R_1^2\left(K_2\left(\frac{MR_1}{\kappa}\right)I_0\left(\frac{MR_2}{\kappa}\right) - I_2\left(\frac{MR_1}{\kappa}\right)K_0\left(\frac{MR_2}{\kappa}\right)\right) + R_2^2\left(K_2\left(\frac{MR_2}{\kappa}\right)I_0\left(\frac{MR_1}{\kappa}\right) - I_2\left(\frac{MR_2}{\kappa}\right)K_0\left(\frac{MR_1}{\kappa}\right)\right)\right], \tag{34}$$

where $I_2\left(\frac{MR_2}{k}\right)$ and $K_2\left(\frac{MR_2}{k}\right)$ are the modified Bessel's functions of first and second kind of order two respectively. The pressure rise ΔP_λ and the friction force on inner and outer tubes $F_\lambda^{(i)}$ and $F_\lambda^{(o)}$, in their non-dimensional forms, are given by:

$$\Delta P_\lambda = \int_0^1 \left(\frac{\partial P}{\partial Z}\right) dZ, \tag{35}$$

$$F_\lambda^{(i)} = \int_0^1 R_1^2\left(-\frac{\partial P}{\partial Z}\right) dZ, \tag{36}$$

$$F_\lambda^{(o)} = \int_0^1 R_2^2\left(-\frac{\partial P}{\partial Z}\right) dZ. \tag{37}$$

3 Perturbation solution

We look for a regular perturbation solution in powers of the small parameter M^2 as follows:

$$W = W_0 + M^2 W_1 + O(M^4), \tag{38}$$

$$U = U_0 + M^2 U_1 + O(M^4), \tag{39}$$

$$P = P_0 + M^2 P_1 + O(M^4), \tag{40}$$

$$F = F_0 + M^2 F_1 + O(M^4). \tag{41}$$

Substituting from equation (38-41) in equation (12), (18) and (21) we get

System of order zero:

$$\frac{1}{R}\frac{\partial(RU_0)}{\partial R} + \frac{\partial W_0}{\partial Z} = 0, \tag{42}$$

$$\frac{\partial P_0}{\partial R} = 0, \tag{43}$$

$$\frac{\partial P_0}{\partial Z} = \frac{\kappa^2}{R}\frac{\partial}{\partial R}\left(R\frac{\partial W_0}{\partial R}\right). \tag{44}$$

with the dimensionless boundary conditions:

$$W_0 = 0, U_0 = 0 \quad \text{at} \quad R = R_1, \tag{45}$$

$$W_0 = 0, U_0 = \frac{\partial R_2}{\partial t} \text{ at } \quad R = R_2. \tag{46}$$

System of order one:

$$\frac{1}{R}\frac{\partial(RU_1)}{\partial R} + \frac{\partial W_1}{\partial Z} = 0, \tag{47}$$

$$\frac{\partial P_1}{\partial R} = 0, \tag{48}$$

$$\frac{\partial P_1}{\partial Z} = \frac{\kappa^2}{R}\frac{\partial}{\partial R}\left(R\frac{\partial W_1}{\partial R}\right) - W_0. \tag{49}$$

with the dimensionless boundary conditions:

$$W_1 = 0, U_1 = 0 \quad \text{at} \quad R = R_1, \tag{50}$$

$$W_1 = 0, U_1 = 0 \text{ at } \quad R = R_2. \tag{51}$$

Zero order solution

Solving equation (44) using boundary conditions (45) and (46), yields:

$$W_0 = \frac{1}{4\kappa^2}\frac{\partial P_0}{\partial Z}\left[R^2 - \left(\frac{(R_2^2 - R_1^2)}{\log\left(\frac{R_2}{R_1}\right)}\right)\log R - \frac{(R_1^2\log R_2 - R_2^2\log R_1)}{\log\left(\frac{R_2}{R_1}\right)}\right] \tag{52}$$

The volume flow rate in the stationary coordinates is given by:

$$F_0 = \int_{R_1}^{R_2} RW_0 dR. \tag{53}$$

Integrating equation (53), with using equation (52), solving the result for $\frac{\partial P_0}{\partial Z}$, we obtain

$$\frac{\partial P_0}{\partial Z} = \frac{-16\kappa^2 F_0 \log\left(\frac{R_2}{R_1}\right)}{B}, \tag{54}$$

where

$$B = (R_2^4 - R_1^4)\log\left(\frac{R_2}{R_1}\right) - (R_2^2 - R_1^2)^2. \tag{55}$$

First order solution

Solving equation (49) using equation (52) and boundary conditions (50), and (51) yields:

$$W_1 = \frac{1}{64\kappa^4}\frac{\partial P_0}{\partial Z}R^4 + \left[\frac{R^2}{4\kappa^2}\frac{\partial P_1}{\partial Z} + \frac{R^2}{16\kappa^4}\frac{\partial P_0}{\partial Z} \times \left(-S\log R - \frac{(R_1^2\log R_2 - R_2^2\log R_1)}{\log\left(\frac{R_2}{R_1}\right)} - S\right)\right] + C_1\log R + C_2, \quad (56)$$

where:

$$C_1 = \frac{(R_2^2-R_1^2)}{4\left(\log\left(\frac{R_2}{R_1}\right)\right)^2\kappa^4}\left[\left(\frac{3(R_2^2+R_1^2)}{16}\log\left(\frac{R_2}{R_1}\right) - \frac{(R_2^2-R_1^2)}{4}\right)\frac{\partial P_0}{\partial Z} - \kappa^2\log\left(\frac{R_2}{R_1}\right)\frac{\partial P_1}{\partial Z}\right],$$

$$C_2 = \frac{-1}{64\left(\log\left(\frac{R_1}{R_2}\right)\right)^2\kappa^4}\{-3(R_1^4(\log R_2)^2 + R_2^4(\log R_1)^2) + 4(R_1^2-R_2^2)(R_1^2\log R_2 - R_2^2\log R_1) + 3(R_2^4+R_1^4)\log R_1\log R_2)\frac{\partial P_0}{\partial Z} - 16\kappa^2\log\left(\frac{R_1}{R_2}\right)(R_1^2\log R_2 - R_2^2\log R_1)\frac{\partial P_1}{\partial Z}\},$$

$$S = \frac{(R_2^2-R_1^2)}{\log\left(\frac{R_2}{R_1}\right)}.$$

The volume flow rate in the stationary coordinates is given by:

$$F_1 = \int_{R_1}^{R_2} RW_1\,dR. \quad (57)$$

Integrating equation (57) with using equation (56), solving the result for $\frac{\partial P_1}{\partial Z}$, we obtain

$$\frac{\partial P_1}{\partial Z} = \frac{1}{C_3}\left[18(R_2^2-R_1^2)F_0\log\left(\frac{R_1}{R_2}\right)\left(\frac{1}{9}(R_1^4-R_2^4-R_1^2R_2^2)\left(\log\left(\frac{R_1}{R_2}\right)\right)^2 + \frac{1}{3}(R_1^2-R_2^2)\log\left(\frac{R_1}{R_2}\right)((R_1^2+2R_2^2)\log R_1 + (R_2^2+2R_1^2)\log R_2 + R_1^2+R_2^2) - R_1^4(\log R_2)^2 - R_2^4(\log R_1)^2 + (R_2^4+R_1^4)\log R_1\log R_2) + \frac{4}{3}(R_2^4-R_1^4)\log\left(\frac{R_2}{R_1}\right) - \frac{2}{3}(R_1^2-R_2^2)^2\right) + 48F_1B\,\kappa^2\left(\log\left(\frac{R_1}{R_2}\right)\right)^2\right], \quad (58)$$

where

$$C_3 = 3B\left[(R_1^4-R_2^4)\left(\log\left(\frac{R_1}{R_2}\right)\right)^2 - (R_1^2-R_2^2)\log\left(\frac{R_1}{R_2}\right)\right].$$

Substituting from equations (54) and (58) in equation (40), then substituting

$$F_0 = F - M^2F_1$$

and neglecting the terms greater than $O(M^4)$, we get:

$$\frac{\partial P}{\partial Z} = \frac{1}{C_3}\left[18(R_2^2-R_1^2)FM^2\log\left(\frac{R_1}{R_2}\right)\left(\frac{1}{9}(R_1^4-R_2^4-R_1^2R_2^2)\left(\log\left(\frac{R_1}{R_2}\right)\right)^2 + \frac{1}{3}(R_1^2-R_2^2)\log\left(\frac{R_1}{R_2}\right)((R_1^2+2R_2^2)\log R_1 + (R_2^2+2R_1^2)\log R_2 + R_1^2+R_2^2) - R_1^4(\log R_2)^2 - R_2^4(\log R_1)^2 + (R_2^4+R_1^4)\log R_1\log R_2 + \frac{4}{3}(R_2^4-R_1^4)\log\left(\frac{R_2}{R_1}\right) - \frac{2}{3}(R_1^2-R_2^2)^2\right)\right] + \frac{16F\kappa^2\log\left(\frac{R_1}{R_2}\right)}{B}. \quad (59)$$

The pressure rise ΔP_λ and the friction force on inner and outer tubes $F_\lambda^{(i)}$ and $F_\lambda^{(o)}$, in their non-dimensional forms, are given by:

$$\Delta P_\lambda = \int_0^1\left(\frac{\partial P}{\partial Z}\right)dZ, \quad (60)$$

$$F_\lambda^{(i)} = \int_0^1 R_1^2\left(-\frac{\partial P}{\partial Z}\right)dZ, \quad (61)$$

$$F_\lambda^{(o)} = \int_0^1 R_2^2\left(-\frac{\partial P}{\partial Z}\right)dZ. \quad (62)$$

4 Separated flow (trapping at the boundary)

A condition frequently used to predict separation in boundary layer theory is to set the vorticity equal to zero on the boundary, setting

$$\xi = \frac{\partial U}{\partial Z} - \frac{\partial W}{\partial R} = 0 \qquad \text{on} \qquad R = R_1, R = R_2 \quad (63)$$

Substituting from equations (22) and (25) into equations (63), we get:

$$\frac{M A_1(Z,t) I_1\left(\frac{M R_1}{\kappa}\right)}{\kappa} - \frac{M A_2(Z,t) K_1\left(\frac{M R_1}{\kappa}\right)}{\kappa} = 0, \quad (64)$$

$$\frac{1}{R_2}\left[\frac{\kappa A_1''(Z,t)\left(R_1 I_1\left(\frac{M R_1}{\kappa}\right) - R_2 I_1\left(\frac{M R_2}{\kappa}\right)\right)}{M} + \frac{\kappa A_2''(Z,t)\left(R_2 K_0\left(\frac{M R_2}{\kappa}\right) - R_1 K_0\left(\frac{M R_1}{\kappa}\right)\right)}{M} + \frac{\frac{\partial^3 p}{\partial z^3}}{2M^2}(R_2^2 - R_1^2)\right] - \frac{M A_1(Z,t) I_1\left(\frac{M R_2}{\kappa}\right)}{\kappa} + \frac{M A_2(Z,t) K_1\left(\frac{M R_2}{\kappa}\right)}{\kappa} = 0. \quad (65)$$

Solving equations (64) and (65) numerically using Newton Raphson method to get separated flow points Z_s on the inner and outer tubes respectively. The normal component of separation points, is given by:

$$R_{2s} = 1 + \frac{\lambda\, k_0\, Z_s}{a_2} + \phi \sin 2\pi(Z_s - t). \quad (66)$$

From equation (25), the vertical velocity component at separation points on the small intestine wall is given by :

$$U_s = -2\pi\phi \cos 2\pi(Z_s - t). \quad (67)$$

5 Numerical results and discussion

To discuss the results obtained above quantitatively, we shall compute the dimensionless pressure rise $\Delta P_\lambda(t)$, and friction force on the inner and outer tubes for different given values of the dimensionless time-mean flow Θ, Jeffrey parameter λ_1, and radius ratio ε. The average rise in pressure $\Delta \bar{P}_\lambda$ is then evaluated by averaging $\Delta P_\lambda(t)$ over one period of the wave. As the integrals in eqs.(35)-(37) are not integrable in the closed form, they are evaluated numerically using a digital computer. Following Srivastava et al. [18], we use the values of various parameters as:. $a_2 = 1.25$ cm., $\lambda = 8.01$cm., $k_0 = \frac{3a_2}{\lambda}$. It may be noted that the theory of wavelength and zero Reynolds number of the present investigation remains applicable here as the radius of the small intestine $a_2 = 1.25$ cm., is small compared with the wavelength $\lambda = 8.01$cm. Furthermore, since most routine upper gastrointestinal endoscopes are between 8 and 11 mm. in diameter, as reported in Cotton and Williams [33] and the radius of the small intestine is 1.25 cm., as reported in Srivastava et al. [18] then the radius ratio ε takes $0.32, 0.38, 0.44$. Equation (35) is plotted in Figures (2-4), and the average rise in pressure is plotted in Figures (5) and (6), eq.(36) is plotted in Figures (7-9) and eq.(37) is plotted in Figures (10-12). Figures (2-4) show that the pressure rise in the case of non - uniform tube increases with increasing radius ratio and it is independent of radius ratio at a certain value of time parameter at $\phi = 0.2, \Theta = 0.05, \lambda_1 = 0.1$, $M = 0.05$ for $\varepsilon = 0.32, 0.38, 0.44$ respectively. Moreover, the pressure rise increases with increasing flow rate at $0 \le t \le 0.08$ and $0.58 \le t \le 1$, but it decreases with increasing flow rate at $0.08 < t < 0.58$ for $\phi = 0.2, \lambda_1 = 0.1, \varepsilon = 0.32, M = 0.05$ and $\Theta = 0, 0.03, 0.05$ respectively. On the other hand, the pressure rise decreases with increasing Jeffrey parameter. Also, the pressure rise is independent of Jeffrey parameter at a certain value of time parameter at $\phi = 0.2, \Theta = 0.05, \varepsilon = 0.32$ and $M = 0.05$ for $\lambda_1 = 0, 0.1, 0.3$ respectively. Figures (2-4) show that the pressure rise in the case of the non-uniform tube is smaller than the corresponding value in the case of the uniform tube. This happens due to the fact that the complete occlusion occurs only at the entry in a diverging tube,whereas in uniform tube, it occurs at all points along the tube. Figures (5) and (6) show that the average of pressure rise increases with increasing radius ratio and it is independent of radius ratio at a certain value of flow rate, the peristaltic pumping, where $\Theta > 0$ (positive pumping) and $\Delta \bar{P}_\lambda > 0$ occurs at $0 \le \Theta < 0.1$, but augmented pumping, where $\Theta > 0$ and $\Delta \bar{P}_\lambda < 0$ (favorable pressure gradient) occurs at $0.1 \le \Theta \le 0.5$ for $\phi = 0.2, \lambda_1 = 0.1$, $M = 0.05$ and $\varepsilon = 0.32, 0.38, 0.44$ respectively. Also, it decreases with increasing Jeffrey parameter and it is independent of Jeffrey parameter at a certain value of flow rate, the peristaltic pumping, occurs at $0 \le \Theta < 0.1$, but augmented pumping, occurs at $0.1 \le \Theta \le 0.5$ for $\phi = 0.2, \varepsilon = 0.32$, $M = 0.05$ and $\lambda_1 = 0, 0.1, 0.3$ respectively. As well as, the average of pressure rise decreases with increasing flow rate where the peristaltic pumping occurs, but it increases with increasing flow rate where augmented pumping occurs for different values of ε and λ_1. Figures (7) and (10) show that the friction forces on the endoscope and on the outer tube has the same direction of wave velocity at $0 \le t < 0.13$ and $0.6 < t \le 1$, but it has the opposite direction of the velocity wave at $0.13 < t \le 0.6$ for $\Theta = 0, 0.03, 0.05$ respectively. Figures (8) and (11) show that the friction forces on the endoscope and on the outer tube increase with increasing radius ratio and they are independent of radius ratio at a certain value of time parameter. Also, the friction force on the endoscope has the same direction of wave velocity at $0 \le t < 0.13$ and $0.6 < t \le 1$, but it has the opposite direction of wave velocity at $0.13 < t \le 0.6$ for $\varepsilon = 0.32, 0.38, 0.44$ respectively. Also, Figures (9) and (12) show that the friction force on outer tube has the same direction of wave velocity at $0 \le t < 0.13$ and $0.6 < t \le 1$, but it has the opposite direction of wave velocity at $0.13 < t \le 0.6$ for $\lambda_1 = 0, 0.3, 0.5$ respectively. Moreover, the friction

forces on the endoscope and the outer tube which have the same direction of wave velocity decrease with increasing flow rate, but the friction forces on the endoscope and on the outer tube which have the opposite direction of wave velocity increase with increasing flow rate. Figures (7-12) show that the friction force on the endoscope is less than that on the outer tube for different values of amplitude ratio, radius ratio and Jeffrey parameter since, there exist degree of occlusion on outer tube, but there is no degree of occlusion on inner tube (endoscope). The friction forces on the endoscope and on the outer tube over uniform tube with the dimensionless time given by equations (36) and (37) are obtained when we put $k_0 = 0$. Figures (7-12) show that the friction forces on the endoscope and on the outer tube in the case of the non-uniform tube is smaller than the corresponding value in the case of the uniform tube [47]-[51].

The numerical results for pressure rise $\Delta P_\lambda(t)$, friction forces on the endoscope and on the outer tube $F^i_\lambda(t)$ and $F^o_\lambda(t)$ is compared with the perturbation results, and both results reveal a very good agreement with each other, as demonstrated in Table 1, Table 2 and Table 3, Figure 2, Figure 3 and Figure 4.

Table 1: Numerical and perturbation solutions for axial pressure rise $\Delta P_\lambda(t)$ for $\phi = 0.2, \lambda_1 = 0.1, \varepsilon = 0.32$, $M = 0.05$ and $\Theta = 0.05$.

t	Numerical solution $\Delta P_\lambda(t)$	Perturbation solution $\Delta P_\lambda(t)$	Error
0	-0.4536349587	-0.4538104934	0.000176
0.25	1.238917493	1.238355137	0.000562
0.5	0.5332983587	0.5333956773	0.000097
0.75	-0.3648230757	-0.365001627	0.000179
1	-0.4536349506	-0.4538104927	0.000176

Table 2: Numerical and perturbation solutions for inner friction force $F^i_\lambda(t)$ for $\phi = 0.2, \lambda_1 = 0.1, \varepsilon = 0.32$, $M = 0.05$ and $\Theta = 0.05$.

t	Numerical solution $F^i_\lambda(t)$	Perturbation solution $F^i_\lambda(t)$	Error
0	0.04645221978	0.0464701945	0.000018
0.25	-0.1268651514	-0.126807566	0.00006
0.5	-0.05460975191	-0.05461971732	0.000009
0.75	0.03735788293	0.0373761666	-0.00001
1	0.04645221894	0.04647019442	0.000018

Table 3: Numerical and perturbation solutions for friction force $F^o_\lambda(t)$ for $\phi = 0.2, \lambda_1 = 0.1, \varepsilon = 0.32$, $M = 0.05$ and $\Theta = 0.05$.

t	Numerical solution $F^o_\lambda(t)$	Perturbation solution $F^o_\lambda(t)$	Error
0	0.8330581003	0.8333358492	0.000278
0.25	-0.7428535314	-0.7429485104	0.000095
0.5	-0.7257503481	-0.7259327379	0.00018
0.75	0.46397148	0.4642582664	0.000287
1	0.8330580632	0.8333358473	0.000278

To discuss the phenomenon of flow separation (trapping) at walls that bound the gap between the endoscope and the small intestine, we have been calculated numerically longitudinal component of separation points on the walls of endoscope and small intestine from equations (64) and (65) respectively by using Mathematica software. Trapping means that a bolus (defined as a volume of fluid bounded by closed streamlines in the wave frame) is transported at the wave speed. The longitudinal component of separation points on the walls versus amplitude ratio are plotted in Figures (13) and (14). To get the normal component of separation points, we have been substituted by the values of longitudinal component at separation points in equation (66). The normal component of separation points versus amplitude ratio are plotted in Figure (15). Also, we have been substituted by the values of longitudinal component at separation points in equation (67) to obtain the normal velocity component of the fluid on the small intestine wall at separation points. The normal velocity component of the fluid at separation points versus amplitude ratio is plotted in Figure (16). The above analysis can be applied in different models such as dynamics of classical and quantum information [50, **?**].

It is clear from Figures (13) and (14) that the longitudinal component of flow separation points on the endoscope and small intestine wall bifurcate into two branches one of them approaches to outlet of contraction region (upper branches) and the other approaches to inlet of contraction region (lower branches) with different values of critical amplitude ratio given as follow: for $\Theta = 0.3$, $\varepsilon = 0.38, \lambda_1 = 0.3$ and $M = 0.05$, critical values of amplitude ratio are $\phi_c = 0.1, 0.08$ (uniform tube), $\phi_c = 0.22, 0.18$ (non-uniform tube), for $\Theta = 0.35$, $\varepsilon = 0.38, \lambda_1 = 0.3$ and $M = 0.05$, critical values of amplitude ratio are $\phi_c = 0.14$, 0.09(uniform tube), $\phi_c = 0.28, 0.22$ (non-uniform tube), and for $\Theta = 0.4$, $\varepsilon = 0.38, \lambda_1 = 0.3$ and $M = 0.05$, critical values of amplitude ratio are $\phi_c = 0.18$, 0.14 (uniform tube), $\phi_c = 0.34, 0.32$ (non-uniform tube)on the endoscope wall and the small intestine wall respectively. Furthermore, Figures(13) and (14) show that an increasing of volume flow rate increases the critical value of amplitude ratio, but it decreases trapping region. The region of flow separation for Z_s increases with increasing volume flow rate for upper branches, but it decreases with increasing volume flow rate for lower branches. In general, from Figures (13) and (14) we can conclude that, trapping region on the endoscope decreases more rapidly than on the small intestine. In addition, the longitudinal component of flow separation points on the endoscope and the small intestine are independent of Hartmann number M, radius ratio ε, and ratio of relaxation time to retardation time λ_1. Figure (15) presents the effects of volume flow rate on the normal component of flow separation points on the small intestine wall at $\Theta = 0.25, M = 0.05$ and $\lambda_1 = 0.3$. It is noted that, normal component of flow separation points on the small intestine wall bifurcate into two branches one of them approaches to outlet of contraction region (upper branches) and the other approaches to inlet of contraction region (lower branches) with different values of critical amplitude ratio given as follow: for $\Theta = 0.3$, $\varepsilon = 0.38, \lambda_1 = 0.3$ and $M = 0.05$, critical values of amplitude ratio are $\phi_c = 0.09$, for $\Theta = 0.35$, $\varepsilon = 0.38, \lambda_1 = 0.3$ and $M = 0.05$, critical values of amplitude ratio are $\phi_c = 0.19$, and for $\Theta = 0.4$, $\varepsilon = 0.38, \lambda_1 = 0.3$ and $M = 0.05$, critical values of amplitude ratio are $\phi_c = 0.24$ on the small intestine wall. The influence of the volume flow rate on the normal velocity component is illustrated in Figure (16) at $\varepsilon = 0.38, M = 0.05$ and $\lambda_1 = 0.3$. From this figure we can

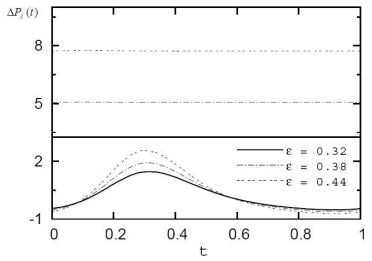

Fig. 2: The pressure rise versus time for $\phi = 0.2, \Theta = 0.05, \lambda_1 = 0.1$ and $M = 0.05$

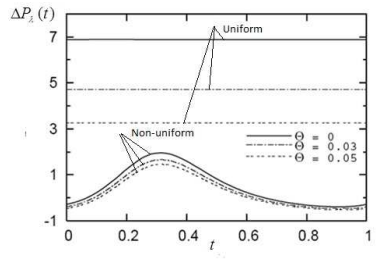

Fig. 3: The pressure rise versus time for $\phi = 0.2, \lambda_1 = 0.1, \varepsilon = 0.32$ and $M = 0.05$

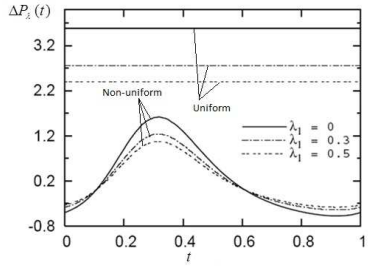

Fig. 4: The pressure rise versus time for $\phi = 0.2, \varepsilon = 0.32, \Theta = 0.05$ and $M = 0.05$

see that, the magnitude of normal velocity component decreases with increasing volume flow rate in contraction region and it increases with increasing amplitude ratio. It is observed that, separation points of the flow in figure (15-16) occur at $\phi = 0.09, 0.19, 0.24$ for $\Theta = 0.3, 0.35, 0.4$ respectively. Also, the positive and negative values of normal velocity component of the fluid show that there exist a portion of fluid towards to forward of contraction region and the other towards to backward of contraction region. Our results agree with these in Srivastava et al.[18] when the radius ratio tends to zero.

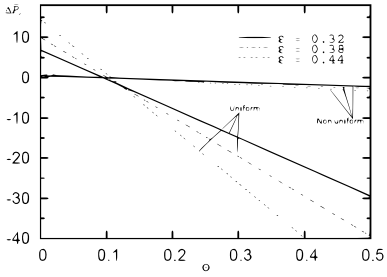

Fig. 5: Effect of radius ratio on average pressure rise for $\phi = 0.2, \lambda_1 = 0.1$ and $M = 0.05$

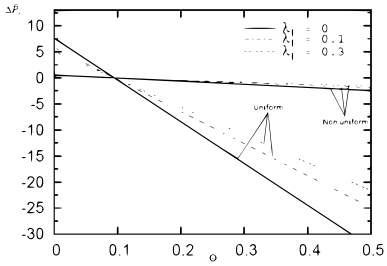

Fig. 6: Effect of Jeffrey parameter on average pressure rise for $\phi = 0.2, \varepsilon = 0.32$ and $M = 0.05$

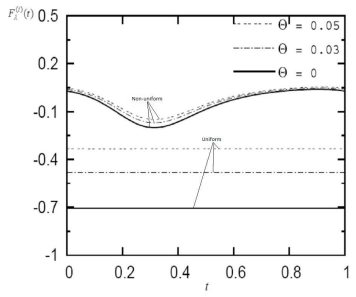

Fig. 7: The friction force on the inner tube (endoscope) versus time for $\phi = 0.2, \varepsilon = 0.32, \lambda_1 = 0.1$ and $M = 0.05$

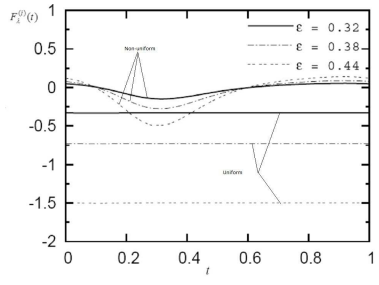

Fig. 8: The friction force on the inner tube (endoscope) versus time for $\phi = 0.2, \lambda_1 = 0.1, \Theta = 0.05$ and $M = 0.05$

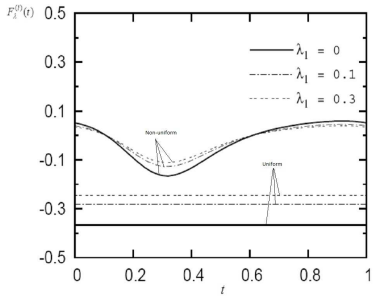

Fig. 9: The friction force on the inner tube (endoscope) versus time for $\phi = 0.2, \varepsilon = 0.32, \Theta = 0.05$ and $M = 0.05$

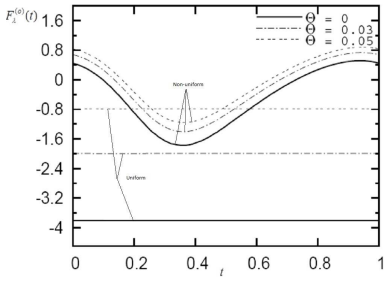

Fig. 10: The friction force on the outer tube versus time for $\phi = 0.2, \varepsilon = 0.32, \lambda_1 = 0.1$ and $M = 0.05$

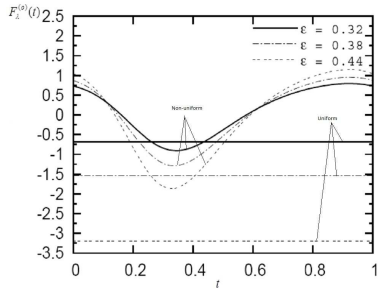

Fig. 11: The friction force on the outer tube versus time for $\phi = 0.2, \lambda_1 = 0.1, \Theta = 0.05$ and $M = 0.05$

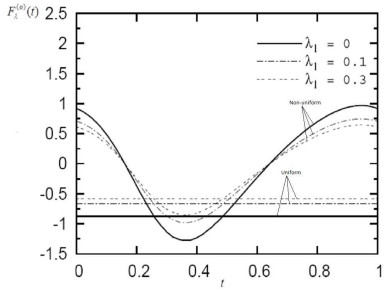

Fig. 12: The friction force on the outer tube versus time for $\phi = 0.2, \varepsilon = 0.32, \Theta = 0.05$ and $M = 0.05$

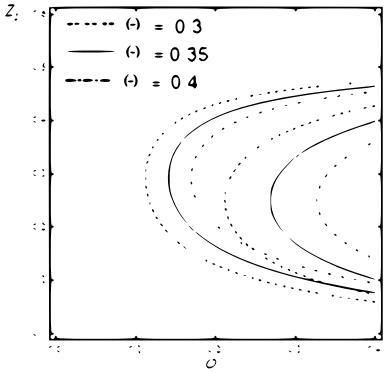

Fig. 13: The longitudinal component of flow separation points on the endoscope versus amplitude ratio for $\lambda_1 = 0.3, \varepsilon = 0.38, t = 0.5$ and $M = 0.05$

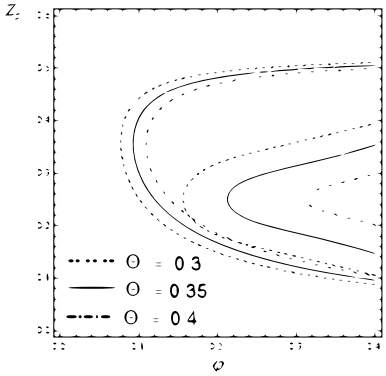

Fig. 14: The longitudinal component of flow separation points on the small intestine wall versus amplitude ratio for $\lambda_1 = 0.3, \varepsilon = 0.38, t = 0.5$ and $M = 0.05$

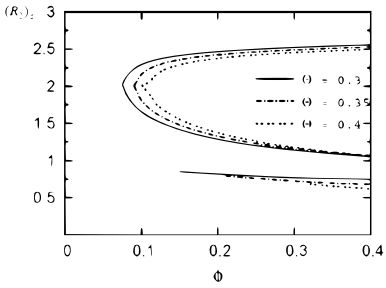

Fig. 15: The vertical component of flow separation points on the small intestine wall versus amplitude ratio for $\lambda_1 = 0.3, \varepsilon = 0.38, t = 0.5$ and $M = 0.05$

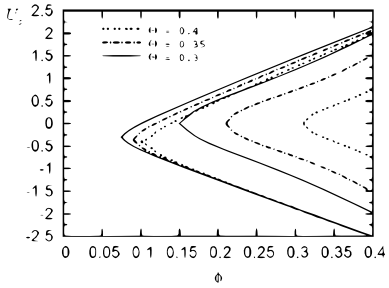

Fig. 16: The radial velocity of flow separation points on the small intestine wall versus amplitude ratio for $\lambda_1 = 0.3, \varepsilon = 0.38, t = 0.5$ and $M = 0.05$

References

[1] H. G. Beger, A. Schwarz, and U. Bergmann, "Progress in gastrointestinal tract surgery: the impact of gastrointestinal endoscopy," Surgical Endoscopy and Other Interventional Techniques, vol. 17, no. 2, pp. 342–350, 2003.

[2] A. Ramachandra Rao, M. Mishra, Peristaltic transport of a power-law fluid in a porous tube, J. Non-Newtonian Fluid Mech. 121 (2004) 163.

[3] M.H. Haroun, Effect of Deborah number and phase difference on peristaltic transport of a third-order fluid in an asymmetric channel, Commun. Nonlinear Sci. Num. Simu. (2007), in press.

[4] V.K. Stud, G.S. Sephon, R.K. Mishra, Pumping action on flow by a magnetic field, Bull. Math. Biol. 39 (1977) 385.

[5] L.M. Srivastava, R.P. Agrawal, Oscillating flow of a conducting fluid with a suspension of spherical particles, J. Appl. Mech. 47 (1980) 196.

[6] H.L. Agrawal, B. Anwaruddin, Peristaltic flow of blood in a branch, Ranchi Univ. Math. J. 15 (1984) 111.

[7] T. Hayat, M. Khan, A.M. Siddiqui, S. Asghar, Non-linear peristaltic flow of a non-Newtonian fluid under effect of a magnetic field in a planar channel, Commun. Nonlinear Sci. Num. Simu. 12 (2007) 910.

[8] M. Kothandapani, S.Srinivas, Peristaltic transport of a Jeffrey fluid under the effect of magnetic field in an asymmetric channel, International Journal of Non-Linear Mechanics 43(2008) 915–924.

[9] Tasawar Hayat, Nasir Ali, Peristaltic motion of a Jeffrey fluid under the effect of a magnetic field in a tube, Communications in Nonlinear Science and Numerical Simulation 13 (2008) 1343–1352.

[10] T. Hayat, Niaz Ahmad, N. Ali, Effects of an endoscope and magnetic field on the peristalsis involving Jeffrey fluid, Communications in Nonlinear Science and Numerical Simulation 13 (2008) 1581–1591.

[11] S. Navaneeswara Reddyal, G. Viswanatha Reddyb, Slip effects on the peristaltic pumping of a Jeffrey fluid through a porous medium in an inclined asymmetric channel, International Journal of Mathematical Archive-4(4), 2013, 183-196.

[12] S. Nadeem, S. Akram, Slip effects on the peristaltic flow of a Jeffrey fluid in an asymmetric channel under the effect of induced magnetic field, Int. J. Numer. Meth. Fluids 2010, 63, 374–394.

[13] M. Sudhakar Reddya, M. V. Subba Reddyb, B. Jayarami Reddyc, and S. Ramakrishnad, Effect of variable viscosity on the peristaltic flow of a Jeffrey fluid in a uniform tube, Advances in Applied Science Research, 2012, 3 (2):900-908.

[14] K. Rajanikanth, S. Sreenadh, Y. Rajesh yadav and A. Ebaid, MHD Peristaltic flow of a Jeffrey fluid in an asymmetric channel with partial slip, Advances in Applied Science Research, 2012, 3 (6):3755-3765.

[15] S. V. H. N. Krishna Kumari P. and M. V. Ramana Murthy, Peristaltic Pumping of a Jeffrey Fluid under the Effect of Magnetic Field in an Inclined Channel, Applied Mathematical Sciences, Vol. 5, 2011, no. 9, 447 - 458.

[16] M.P. Wiedeman, Dimensions of blood vessels from distributing artery to collecting vein, Circ. Res. 12 (1963) 375.

[17] J.S. Lee, Y.C. Fung, Flow in non-uniform small blood vessels, Microvasc. Res. 3 (1971) 272.

[18] L.M. Srivastava, V.P. Srivastava, S.N. Sinha, Peristaltic transport of a physiological fluid: I. Flow in non-uniform geometry, Biorheology 20 (1983) 153.

[19] J.C. Misra, S.K. Pandey, Peristaltic transport in a tapered tube, Math. Comput. Modelling 22 (1995) 137.

[20] E.F. Elshehawey, A.M. El Misery, A.H.A. El Naby, Peristaltic motion of generalized Newtonian fluid in a non-uniform channel, J. Phys. Soc. Japan. 67 (1998) 434.

[21] Kh.S. Mekheimer, Peristaltic flow of blood under effect of a magnetic field in a non-uniform channels, Appl. Math. Comput. 153 (2004) 763.

[22] E.F. Elshehawey, A.R. El Saman, M. El Shahed, M. Dagher, Peristaltic transport of a compressible viscous liquid through a taperedpore, Appl. Math. Comput. 169 (2005) 526.

[23] Kh.S. Mekheimer, Peristaltic transport of a Newtonian fluid through a uniform and non-uniform annulus, Arab. J. Sci. Eng. 30 (2005) 69.

[24] A. H. Shapiro, M.Y. Jaffrin, S. L. Weinberg, "Peristaltic pumping with long wavelengths at low Reynolds number", J. Fluid Mech. 37 (1969) 799.

[25] S. Takabatake, K. Ayukawa, A. Mori, "Peristaltic pumping in circular cylindrical tubes: a numerical study of fluid transport and its efficiency", J. Fluid Mech. 193 (1988) 267–283.

[26] A.M. Siddiqui, A. Provost, W. H. Schwarz, "Peristaltic pumping of a second-order fluid in a planar channel", Rheol. Acta 30 (1991) 249.

[27] A. M. Siddiqui, W. H. Schwarz, "Peristaltic motion of a third-order fluid in a planar channel", Rheol. Acta 32 (1993) 47.

[28] A. M. Siddiqui, W. H. Schwarz, Peristaltic flow of a second-order fluid in tubes, J. Non-Newtonian Fluid Mech. 53 (1994) 257.

[29] M. Mishra, A. R. Rao, "Peristaltic transport of a Newtonian fluid in an asymmetric channel", ZAMP 54 (2003) 532–550.

[30] Abd El Hakeem Abd El Naby, A. E. M. El Misery, M. F. Abd El Kareem, "Separation in the flow through peristaltic motion of a Carreau fluid in an uniform tube", J. Phys. A: Statist. Mech. Appl. 343C (2004) 1–14.

[31] Abd El Hakeem Abd El Naby, A. E. M. El Misery, M. F. Abd El Kareem, "Effects of a magnetic field on trapping through peristaltic motion for generalized Newtonian fluid in channel", J. Phys. A (2006) 79–92.

[32] Abd El Hakeem Abd El Naby, M. F. Abd El Kareem, "The Flow Separation through Peristaltic Motion for Power-law Fluid in Uniform Tube", J. Appl. Math. Sciences, Vol. 1, 2007, no. 26, 1249 - 1263.

[33] P. B. Cotton and C. B. Williams, Practical Gastrointestinal Endoscopy, London: Oxford University Press Third Edition, (1990).

[34] T. Hayat, N. Ahmad and N. Ali, Effects of an endoscope and magnetic field on the peristalsis involving Jeffery Fluids, Communications in Nonlinear Science and Numerical Simulation 13(8):1581-1591, (2008)

[35] A. M. Abd-Alla, S. M. Abo-Dahab, M. A. Abdelhafez and Y. Elmhedy, Effect of heat and mass transfer on the nanofluid of peristaltic flow in a ciliated tube, Scientific Reports volume 13, Article number: 16008 (2023)

[36] D. Vernardou, and A, Kazas, and M. Apostolopoulou, and N. Katsarakis, and E. Koudoumas, Hydrothermal Growth of MnO2 at 95 oC as an Anode Material, International Journal of Thin Film Science and Technology, Vol. 5 No. 2 pp. 121-127 (2016), http://dx.doi.org/10.18576/ijtfst/050207

[37] M. s. Al-Qrinawi, and T. M. El-Agez, and M. S. Abdel-Latif, and S. A. Taya, Capacitance-voltage measurements of hetero-layer OLEDs treated by an electric field and thermal annealing, International Journal of Thin Film Science and Technology, 10, No. 3, 217-226 (2016) http://dx.doi.org/10.18576/ijtfst/100311

[38] Y, Quintana, and W. Ram??rez, and A. Urieles, Euler Matrices and their Algebraic Properties Revisited, Appl. Math. Inf. Sci. 14 (2020) 583-596: doi:10.18576/amis/140407

[39] V. Joshi, and M. Kapoor, A Novel Technique for Numerical Approximation of 2 Dimensional Non-Linear Coupled Burgers Equations using Uniform Algebraic Hyperbolic (UAH) Tension B-Spline based Differential Quadrature Method, Appl. Math. Inf. Sci. 15, (2021) PP: 217–239, doi:10.18576/amis/150215

[40] K. Moaddy, Reliable Numerical Algorithm for Handling Differential- Algebraic System Involving Integral-Initial Conditions, Appl. Math. Inf. Sci. 12 (2018) 317-330: doi:10.18576/amis/120206

[41] A. A. Elhadary, and A. El-Zein, and m. Talaat, and G. El-Aragi, and A. El-Amawy, Studying The Effect of The Dielectric Barrier Discharge Non- thermal Plasma on Colon Cancer Cell line, International Journal of Thin Film Science and Technology, Vol. 10 No. 3 pp. 161-168 (2021), http://dx.doi.org/10.18576/ijtfst/100305

[42] M. Shapaan, DC Conductivity, Thermal Stability and Crystallization Kinetics of the Semiconducting 30P2O5 (50-x)V2O5 xB2O3 20Fe2O3 Oxide Glasses. International Journal of Thin Film Science and Technology, Vol. 5 No. 3 pp. 143-153 (2016) http://dx.doi.org/10.18576/ijtfst/050301

[43] V. . Sanap, and B. H. Pawar, Influence of annealing temperature on properties of nanocrystalline CdO thin films synthesized via thermal oxidation process, International Journal of Thin Film Science and Technology, Vol. 2 No. 2 pp. 107-111 (2013), http://dx.doi.org/10.12785/ijtfst/020206

[44] S. Thota, and S. D. Kumar, A New Reduction Algorithm for Differential-Algebraic Systems with Power Series Coefficients, Inf Sci. Lett. 10 (2021) 59-66: doi:10.18576/isl/100108

[45] S. Thota, Implementation of a Reducing Algorithm for Differential-Algebraic Systems in Maple, Inf. Sci. Lett. 10, (2021) 263-266: doi:10.18576/isl/100210

[46] Y. Liu, Extended Bayesian Framework for Multicategory Support Vector Machine, J. Stat. Appl. Prob. 9 (2020) 1-11: doi:10.18576/jsap/090101

[47] I. M. Ibrahim, Characterization and gas sensitivity of cadmium oxide thin films prepared by thermal evaporation technique, International Journal of Thin Film Science and Technology 1 (2012), pp. 1-9

[48] J. K. Das, and M. A. I. Nahid, Electrical Properties of Thermal Evaporated Bismuth Telluride Thin Films, International Journal of Thin Film Science and Technology, Vol. 4, No.1, 13-16 (2015) http://dx.doi.org/10.12785/ijtfst/040103

[49] M. Kumar, and A. A. Awasthi, and A. Kumar, and K. K. Patel, Sequential Testing Procedure for the Parameter of Left Truncated Exponential Distribution, J. Stat. Appl. Prob. 9 (2020), 119-125: doi:10.18576/jsap/090111

[50] A. Redwan, and A.H. Abdel-Aty, and N. Zidan, and T. El-Shahat, Dynamics of Classical and Quantum Information on Spin-chains with Multiple, Inf. Sci. Lett. Vol. 7, No.2 (2018) PP. 29-33 DOI: http://dx.doi.org/10.12785/isl/070201

[51] R. Sridevi, and P. Philominathan, Quantum Colour Image Encryption Algorithm Based on DNA and Unified Logistic Tent Map, Inf. Sci. Lett. Vol. 9 No. 3 (2020) PP. 219-231 DOI: http://dx.doi.org/10.18576/isl/090309

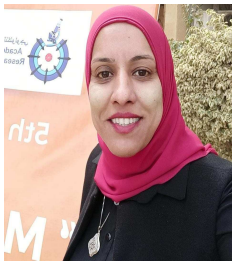

E. G. El-Hadidy is currently an lecturer in the Department of Mathematics, Faculty of Science, Damietta University, Egypt. She has contributed significantly in the area of Quantum information and its applications. She has published several research articles in various leading journals.

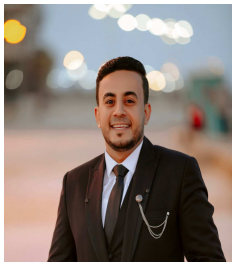

Mohamed Ibrahim received a B.Sc. degree in science majoring in mathematics from the Faculty of Science, Damietta University, Damietta, Egypt in 2016, received a M.Sc. degree in science majoring in mathematics from the Faculty of Science, Damietta University, Damietta, Egypt in 2022, and he was a assistant lecturer at the Department of Mathematics, Faculty of Science, Damietta University, Damietta, Egypt.

Abd El Hakeem Abd El Naby is currently an Associate Professor in the Department of Mathematics, Faculty of Science, Damietta University, Egypt. He has contributed significantly in the area of modelling and analysis of fluid mechanics and its applications. He has published several research articles in various leading journals.